ISSN 2816-573X

ORIGINAL ARTICLE

In vitro Anti-Cancer Effect of Polymeric Nanoparticles Encapsulating *Caralluma tuberculata* in Cancer Cells

Mahnoor Fayyaz[1,2], Usama Sarwar[2], Farwa Nurjis[2], Joham Sarfraz Ali[3], Sobia Tabassum[1], Abida Raza[4*]

Fayyaz M, Sarwar U, Nurjis F et al. In vitro Anti-Cancer Effect of Polymeric Nanoparticles Encapsulating Caralluma tuberculata in Cancer Cells. Int J Adv Nano Comput Anal. 2023;2(1):22-38.

Abstract

Rapidly evolving drug delivery systems employ therapeutic agents (liposomes, polymers, and nanospheres) to achieve optimum therapeutic and targeted effects with declined side effects to cure chronic diseases like cancer. Nano-formulation of a natural product i.e., *Caralluma tuberculata* (Ct) extract, has been used as an effective combinational therapy with enhanced biocompatibility owing to its strong anti-oxidant, anti-inflammatory, anti-bacterial, and anti-tumor potential. Ct extract was prepared using three solvents (EtOH, MeOH, and $CHCl_3$) amongst which methanolic Ct extract exhibited the highest percentage yield (9.6%). Qualitative phytochemical screening, thin layer chromatography (TLC), and antioxidant assays (DPPH assay and H_2O_2 assay) were performed. The percentage free radical scavenging values were found to be 86.25% (IC_{50}=140.1 µg/ml) and 88% (IC_{50}=14.22 µg/ml) at 1000 µg/ml concentration for both assays respectively. Methanolic Ct extract was then encapsulated in chitosan-tripolyphosphate (CS-TPP) nanoparticles using ionic gelation method with an encapsulation efficiency of 87%. Characterization showed uniform size distribution of 140 nm particle size using DLS and encapsulation of Ct extract inside CS-TPP nanoparticles was confirmed by UV spectrophotometry and FTIR. Ct loaded CS-TPP nanoparticles showed less than or equal to 5% hemolytic activity at concentrations of 15.62 µg/ml, 31.25 µg/ml, 62.5 µg/ml, and 125 µg/ml, suggesting its safer usage at lower concentration. Rhodamine conjugated Ct loaded CS-TPP nanoparticles showed significant uptake efficiency in breast cancer cells compared to control. Ct extract and the nanoformulation were treated against triple negative breast cancer cell lines (CAL-51) for the evaluation of cytotoxicity exhibiting 30-40% (IC_{50}=122.3 µg/ml) and up to 75% (IC_{50}=14.39 µg/ml) cytotoxicity respectively. The study paves way for the encapsulation of medicinal plants in polymeric nanoparticles to achieve safer and highly efficient drug delivery systems.

Key Words: *Caralluma tuberculata; Antioxidant; Anticancer; Nanoparticles; Biocompatibility*

[1]*Department of Biological Sciences, International Islamic University, Islamabad 44000, Pakistan*

[2]*NILOP Nanomedicine Research Laboratories, National Institute of Lasers and Optronics College (NILOP-C), Pakistan Institute of Engineering and Applied Sciences, Nilore, Islamabad 45650, Pakistan*

[3]*Department of Biological Sciences, National University of Medical Sciences, Islamabad 46000, Pakistan*

[4]*National Centre of Industrial Biotechnology, Pir Mehr Ali Shah Arid Agriculture University, Rawalpindi, 46000, Pakistan*

[*]*Corresponding author: Abida Raza, Technical Director, National Center of Industrial Biotechnology, University Institute of Biochemistry and Biotechnology, Pir Mehr Ali Shah Arid Agriculture University, Rawalpindi, Pakistan, Tel: +923457713910; E-mail: abida_rao@yahoo.com*

Received: May 15, 2023, Accepted: June 21, 2023, Published: July 11, 2023

Introduction

Nano-delivery systems are a rapidly evolving science in which molecules are used for the efficient and targeted delivery of therapeutic agents to achieve optimum therapeutic effects [1]. The encapsulated therapeutic agents of varying nature and properties, such as liposomes, polymers, micelles, and nanospheres, are prepared to enhance the therapeutic effect and minimize the adverse side effects associated with other drugs. The targeted and site-specific drug delivery approach is employed to treat many chronic human diseases [2].

Nanostructures are preferred as the carrier in the drug delivery systems because these substances tend to stay in the circulatory system for a longer period of time. Also, the drug release at the site of interest is controlled and specified. Resultantly, the adverse side effects can be circumvented. The extremely small size of these drug carriers enables them to penetrate through the tissues and be easily taken up by the cells at the target site, thus entertaining an efficient delivery system [3,4]. The efficacy and efficiency of these structures may vary according to their size, conformation, biophysical and chemical characteristics. Polymeric nanoparticles, for example, have proven to be efficient drug carriers owing to their size i.e. 10 to 1000 nm [5]. Studies show that targeted drug therapy through nanoparticles is a notable approach in reducing the problem of recurrence and drug side effects reportedly associated with different cancer therapies [6,7].

Synthesis of nanoparticles from natural sources for different therapies embraces many benefits such as biodegradability, biocompatibility and bioavailability. These nanoparticles, due to their low toxicity, bioavailability and stability are used as nano carriers for the drug encapsulation and drug delivery against different cancer cells [8]. Biocompatible nanoparticles are preferred since they deliver the drug to its targeted tumour cell and offer less cytotoxicity [9]. Different nanoformulations in the form of liposomes, polymers and nanoemulsions are widely used for the delivery of the drug to its target [1,10]. Chitosan, a biopolymer has gained interest as a nano carrier because of its biocompatibility, biodegradability and non-toxicity. According to reported studies, chitosan nanoparticles (CS-NPs) are also successfully tested in different in vitro and in vivo studies in case of cancer [11,12]. Application of CS-NPs to the tumour cells enhances the chance of uptake of drug carrier by the cells [13,14]. It also helps them in targeted delivery of drug to the cancer cells due to their stability for longer time in blood stream without any structural changes [15].

Caralluma tuberculata (Ct) is a medicinal plant belonging to the family Apocynaceae, present in abundance across South Asia, Africa and Middle East [16]. The vernacular name for Ct is “chunga” or “chung” and is eaten as a vegetable in Punjab and Khyber Pakhtun Khwa, Pakistan. The characteristic features of Caralluma species is the absence of leaves and a fleshy stem with grooves on it [17]. The 4-angled stem is erect with small, dark-colored flowers on it [18,19]. Ct constitues a wide range of phytochemicals including cardiac glycosides (pregnane glycosides; C_{21} chain), steroids, saponins, flavonoids and phenols [20]. Plants of the Caralluma genus have been of wide interest to the researchers owing to its strong medicinal properties such as anti-inflammatory, anti-tumor, anti-oxidant, anti-arthritic, as well as analgesic activity [21].

A study performed by Ahmed et al., 2015 concluded that methanolic extracts of Ct have cytotoxic effect against different types of cancer cells. Ethanolic extract of Caralluma species has been found to have significant cytotoxic effect against colon and lung cancer cells [22,23]. Various pregnane glycosides isolated from Ct extracts show cytotoxic effect when tested against different human cell lines [24]. Ethyl acetate extract of Ct has proven to be the

most effective anti-proliferative agent against breast cancer cells. It has been established that this apoptotic effect is due to the presence of pregnane glycosides so this plant could be used in the formulation of anti-cancer drugs [25,26]. Moreover, studies conducted to check the acute and chronic toxicity of various concentrations of Ct extracts on albino mice over a period of 90 days have shown that these extracts are completely non-toxic (safe) and biocompatible. No growth inhibition or development retardation was observed [27]. Numerous studies have established that cardiac glycosides have the potential of inducing apoptosis in cancer cells by elevating the intracellular Ca^{2+} levels, since these phytochemicals are responsible for inhibiting Na^{+}/K^{+} ATPase pathway [28]. Studies have established that altering the intracellular calcium homeostasis affects both cell proliferation and cell death, in ovarian, prostate, brain and breast cancer cells [29]. This could be explained by the underlying mechanism i.e., the interaction of tumor necrosis facror (TNF), related to Ca^{2+} levels in the cell, with the death receptor (DR4) inducing tumor cell death [30].

The purpose of this study was to prepare chitosan nanoparticles encapsulating Ct, and check its cytotoxicity via MTT assay against triple negative triple negative breast cancer cells. For this purpose, we have performed the qualitative phytochemical screening of the methanolic Ct extract and evaluated its antioxidant potential. The nano-formulation synthesis was confirmed by UV-Vis spectrophotometer, Fourier-transform infrared spectroscopy (FTIR), particle imaging, particle size and zeta potential measurement. Fluorescence intensity was also determined to assess the loading of Rhodamine dye in the formulation. The biocompatibility of the prepared nanoparticles was checked via the haemolytic assay prior to exposure followed by evaluation of anticancer effect on breast cancer cells.

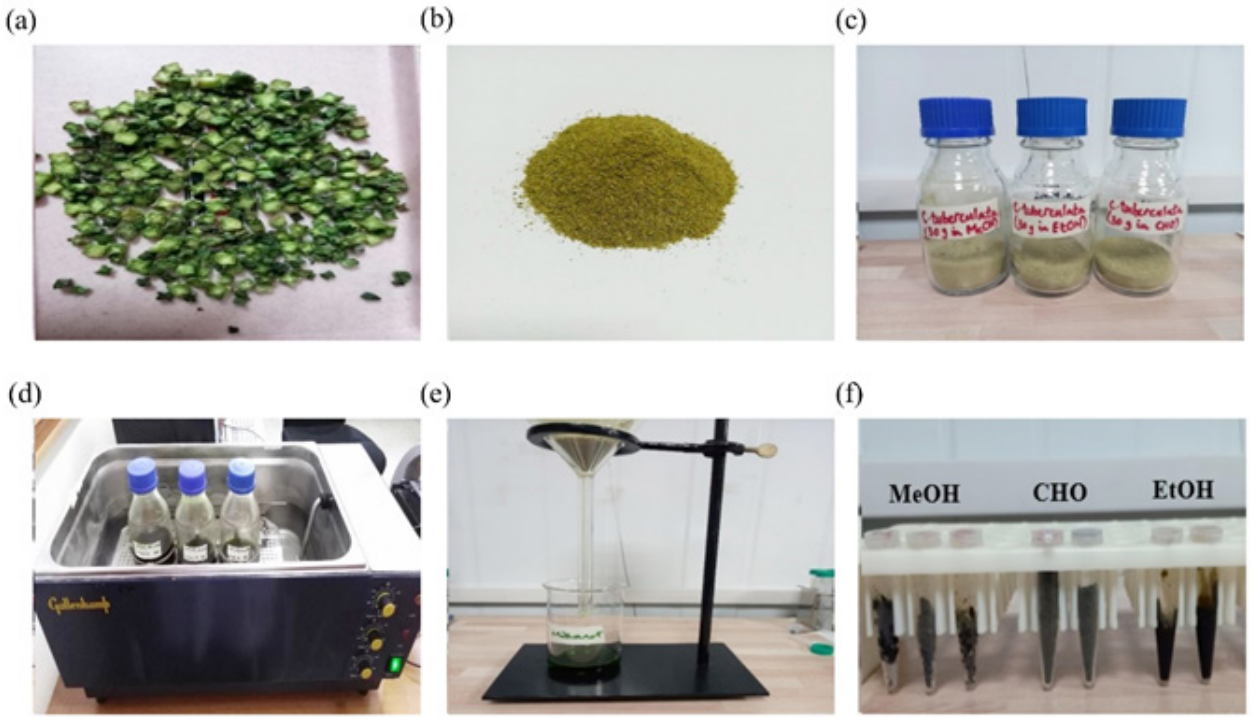

Figure 1) ***Preparation of Ct extract by maceration method*** *(a) Collection and drying (b) 90g grinded powder in airtight bag (c) Powdered 30g in each autoclaved reagent bottle (d) Reagent bottles placed on shaker (e) Filtration of solvents (f) Prepared extracts stored in Eppendorf tubes (Methanol, Chloroform and Ethanol extractThe percentage yield of all the prepared Ct extracts was calculated by the following formula:Percentage Yield=(Crude extract weight)/ (Dry plant weight) × 100.*

Material and Methods

Materials

The chemicals used during the study are mentioned in supplementary data.

Plant Collection and Extraction

The plant Ct N. E. Brown was collected from Quetta, Balochistan, Pakistan in November 2019. The plant material was identified and authenticated (IIUDES 1102) by Dr. Muhammad Ibrar Shinwari, Associate Professor, Department of Environmental Sciences, International Islamic University, Islamabad. The extraction procedure is mentioned in supplementary data and represented in Figures 1a to 1f.

The percentage yield of all the prepared Ct extracts was calculated by the following formula:

Percentage Yield=(Crude extract weight)/(Dry plant weight) × 100

Qualitative Phytochemical Tests

Ct extract solution (2 mg/ml) was prepared in methanol and screened for qualitative phytochemicals tests to check the presence of phenols, cardiac glycosides, steroids, flavonoids, tannins and terpenoids according to a previously described protocol [31,32], with few modifications. Similar assays were performed for the Ct loaded nanoparticles synthesized through procedure stated further.

Thin Layer Chromatography (TLC)

Thin Layer Chromatography was employed to analyse the various classes of phytochemicals (flavonoids, cardiac glycosides, steroids) present in the Ct extract following a pre-suggested protocol [33]. The detailed procedure for flavonoids and their glycosides, cardiac glycosides and steroids is mentioned in supplementary data. Different classes of aforementioned secondary metabolites were tested later on by measuring the Rf values of the obtained bands after using different visualizing agents.

Antioxidant Assays

DPPH (1, 1-diphenyl-2-picryl-hydrazyl) free radical scavenging assay

The DPPH free radical scavenging assay was carried out by using the standard procedure as described earlier [34,35] with a few changes. The procedure of DDPH assay is stated in supplementary data. Antioxidant capacity was determined by the following formula:

Inhibition (%)=(Abs of control-Abs of sample)/(Abs of control) × 100

Hydrogen peroxide radical scavenging assay

The capacity of the Ct extract to quench H_2O_2 was evaluated by conducting the experiment according to [36] with slight modifications. The detailed procedure is mentioned in supplementary data. The scavenging ability of H_2O_2 was calculated using the formula:

Inhibition (%)=(Abs of control-Abs of sample)/(Abs of control) × 100

CS-TPP nanoparticle synthesis

CS-TPP nanoparticles were synthesized employing the ionic gelation method [37]. Briefly, chitosan was dissolved in 1% acetic acid solution to prepare 0.1% chitosan solution under magnetic stirring at 500 rpm overnight. The TPP solution (1%) was prepared in distilled water. Nanoparticle formation was achieved by the addition of 1ml TPP into 10 ml CS solution. This mixture was subjected to constant magnetic stirring (500 rpm) at room temperature for 30 min. afterwards, centrifugation at 10,000 rpm was done for 1 hour. The pellet was re-suspended in distilled water three times followed by ultra-sonication (3 mm probe, Sonics Vibra cell; Sonics & Material, Inc., USA) at 80% pulser ratio, 55 seconds ON, 5 seconds OFF. The sample was lyophilized and kept at 4°C for further use, as shown in Figure 2a.

Ct loaded nanoparticle synthesis

CS-TPP nanoparticles were synthesized

employing the ionic gelation method [37]. First, 1g of Ct extract was dissolved in 1ml TPP solution (1%). The mixture was added into the CS solution followed by magnetic stirring for 30min at 500rpm. Centrifugation, washing, and sonication was performed. The sample was lyophilized and kept at 4°C, as shown in (Figure 2b). Encapsulation efficiency (%) was calculated by the following formula:

Encapsulation efficiency=(Plant added-Plant encapsulated)/ (Plant added) × 100

Rhodamine conjugated Ct loaded nanoparticle synthesis

Ct loaded CS-TPP nanoparticles were synthesized employing the ionic gelation method. Rhodamine green dye was conjugated with the nanoparticles. Stock solution (1 µg/ml) of rhodamine green was prepared. First, 1g of Ct extract was dissolved in 1ml TPP solution (1%) followed by addition of 10µl rhodamine green dye. The mixture was then added into the chitosan solution followed by magnetic stirring for 30min at 500rpm. Centrifugation, washing, and sonication was performed. The sample was lyophilized and kept at 4°C for use.

Characterization of nanoparticles

For characterization of synthesized nanoparticles, Dynamic Light Scattering (DLS), Cell imaging, FTIR analysis and the UV spectrophotometry were used, and its details are mentioned in supplementary data.

Biocompatibility study

In vitro haemolytic assay for Ct extract and Ct loaded CS-TPP nanoparticles was performed following the protocol explained earlier [38,39], with slight modifications. Fresh blood (5cc) was derived from a human volunteer and collected into a sterile vacutainer. Centrifugation was done at 14000rpm for 10min at 4°C to separate the plasma. The Eppendorf was washed three times with phosphate-buffered saline (PBS) (pH 7.2) solution. The volume was made up with PBS in a falcon tube such that the blood suspension was 2% of the whole volume. A series of concentrations for each sample were taken i.e., 15.62 µg/ml to 1000 µg/ml. Equal volumes of the sample were incubated with the blood suspension in water bath at 37°C for 1hour. Plasma was collected via centrifugation at 15000rpm for 10min. The absorbance was measured at 540 nm using microplate reader (Model FLx800; Biotek, VA, USA). Triton X-100 (10%) was kept as positive control. Red blood cells were kept as the negative control. The percentage of haemolysis was calculated using the following formula.

Hemolysis (%)=(Abs of sample-Abs of negative control)/ (Abs of positive control-Abs of negative control) × 100

Cellular uptake study

Triple negative breast cancer cells were collected and seeded in a 24 well plate with 600µl per well and incubated for 24h according to the protocol [40]. The cells were washed with PBS thoroughly after removing the media. Ct loaded CS-TPP nanoparticles with and without rhodamine dye were diluted with PBS to 100 µg/ml. Nanoparticles (300µl) were added to each well and incubated for 30min. Afterwards, the cells were washed with PBS thrice followed by addition of 4% paraformaldehyde (300µl) and incubation for 15min to fix the cells. After removing the paraformaldehyde, staining of the nucleic acid was achieved by addition DAPI solution (100µl, 100ng/ml) for 15min. again, the cells were washed with PBS twice. The fluorescence of the cells was observed using cell imager (Evos® FL Cell Imaging System; Thermo Fisher Scientific, MA, USA).

Cytotoxicity assay

The synthesized nanoformulation was tested for its anti-cancer activity against triple negative breast cancer cell lines. The cytotoxicity of the Ct extract and Ct-loaded CS-TPP nanoparticles was assessed by performing the MTT assay [41]. Triple negative breast cancer cell lines were seeded at a density of 3×10^4 cells in Dulbecco's Modified Eagle Media (DMEM), supplemented with 10% Fetal Bovine Serum

(FBS). Further supplementation was done with penicillin and streptomycin antibiotics. The cells were maintained at 37°C in 5% CO_2 incubator. Trypsinization was performed to harvest the cells at room temperature. Cells were exposed to varying concentrations of Ct extract and Ct-loaded CS-TPP nanoparticles and were incubated in 5% CO_2. An exposure period of 24 hour is given after which 10µl of MTT solution (5 mg in 1ml of PBS) (Sigma Aldrich, USA) was added to the culture plates. The plates were then incubated at 37°C for 4 hour. Plates were analysed using microplate reader microplate reader (Model FLx800; Biotek, VA, USA) and the absorbance was measured at 570 nm. The percentage cell viability was calculated using the following formula.

Cell Viability (%)=(Absorbance of sample-Absorbance of blank)/ (Absorbance of control-Absorbance of blank) × 100

Statistical Analysis

All the experiments were performed in triplicates. The latest version of Graph Pad Prism 9.1.0 was used for the statistical analysis. Data represented as mean ± SD and $p< 0.05$ was considered significant.

Results

Among the three extracts, the methanolic Ct extract gave the maximum yield of 9.6% whereas the ethanolic and chloroform Ct extracts showed a percentage yield of 6.26% and 4.8% respectively. Hence, the methanolic Ct extract was used (Figure 2).

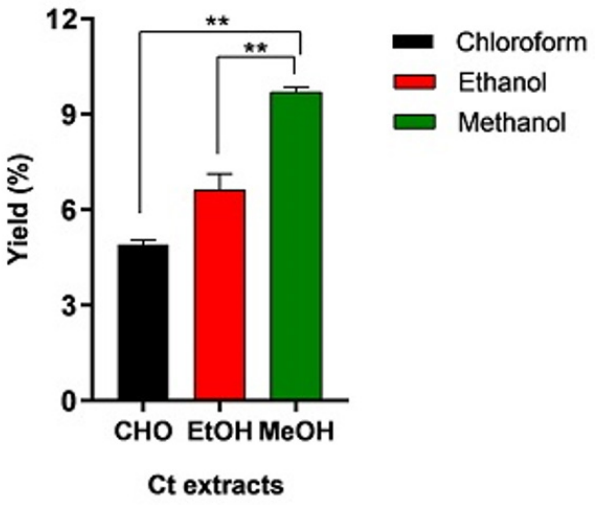

Figure 2) *Percentage yield of Ct extracts. A significant difference ($p<0.001$) in the percentage yield of all solvents has been found but methanolic extract provides a maximum yield of up to 9.6%.*

Qualitative Phytochemical Analysis

The methanolic Ct extract was tested for six phytochemicals i.e. flavonoids, phenols, tannins, terpenoids, steroids and cardiac glycosides. The results shown in (Figure 3) state the presence of all the phytochemicals except for terpenoids and phenols.

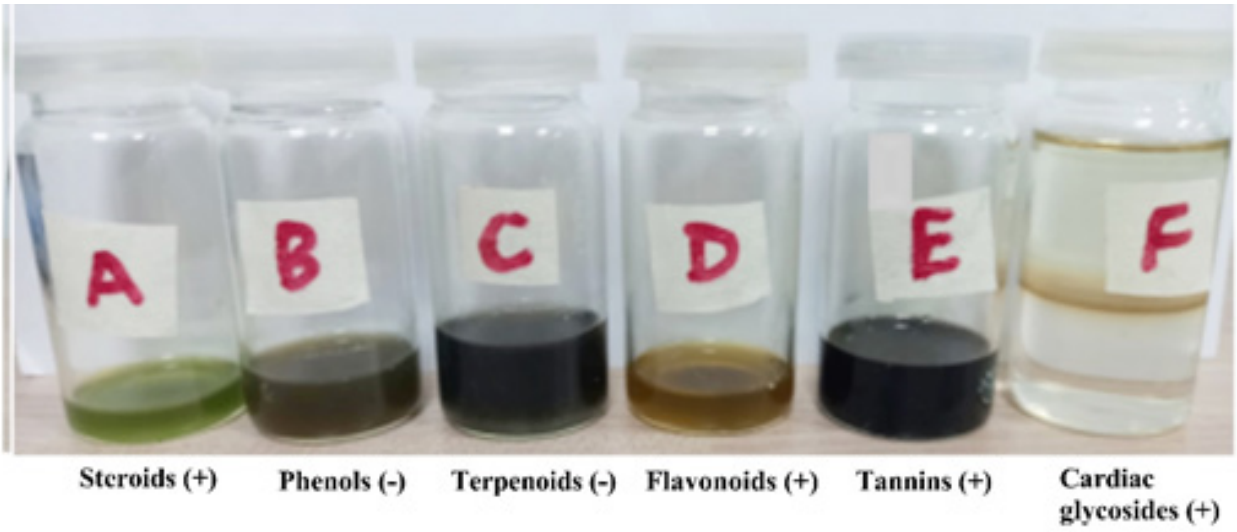

Figure 3) *Qualitative Phytochemical Tests of methanolic extracts of Ct tested against various classes of secondary metabolites. The "+" sign indicates presence and "–" sign indicates absence of a particular class.*

TABLE 1
Confirmatory tests for various phytochemicals in different solvent systems.

Phytochemicals	Solvent Systems	Confirmatory Tests
Flavonoids and their glycosides	Chloroform: Methanol 7:3	3% boric acid + 10% oxalic acid spray
Cardiac glycosides	Ethyl acetate: Methanol: Water 81:11:8	10% KOH + 50% MeOH solution spray
Saponins and steroids	Ethyl acetate: Methanol: Water 81:11:8	10% H_2SO_4 spray

Thin layer chromatography (TLC)

The results of TLC for methanolic Ct extract are shown in (Table 1). The TLC plates were observed under UV for visualization (Figures 4a and 4b). It showed the presence of all tested secondary metabolites. The sample run in chloroform and methanol solvent system clearly showed the presence of flavonoids and their glycosides with Rf value of 0.77. Appearance of creamy white color on the plate after the spray of boric acid and oxalic acid further confirmed the presence of flavonoids and their glycosides. The sample run in ethyl acetate, methanol and water solvent system clearly showed the presence of cardiac glycosides with Rf value of 0.83. Appearance of reddish grey spots on the plate after the spray of potassium hydroxide and methanol further confirmed the presence of cardiac glycosides. The sample run in ethyl acetate, methanol and water solvent system clearly showed the presence of saponins and steroids with Rf value of 0.84. Appearance of reddish-brown spots on the plate after the spray of sulfuric acid further confirmed the presence of saponins and steroids.

DPPH free radical scavenging assay

Anti-oxidant activity of a series of concentrations of methanolic Ct extract was measured by DPPH free radical scavenging assay. Figure 5a shows that antioxidant activity of methanolic Ct extract compared with standard ascorbic acid. Results showed that a percentage inhibition of 86.25% was exhibited at a concentration of 1000 µg/ml indicating strong antioxidant activity. The IC_{50} value calculated was 140.1 µg/ml for the methanolic Ct extract.

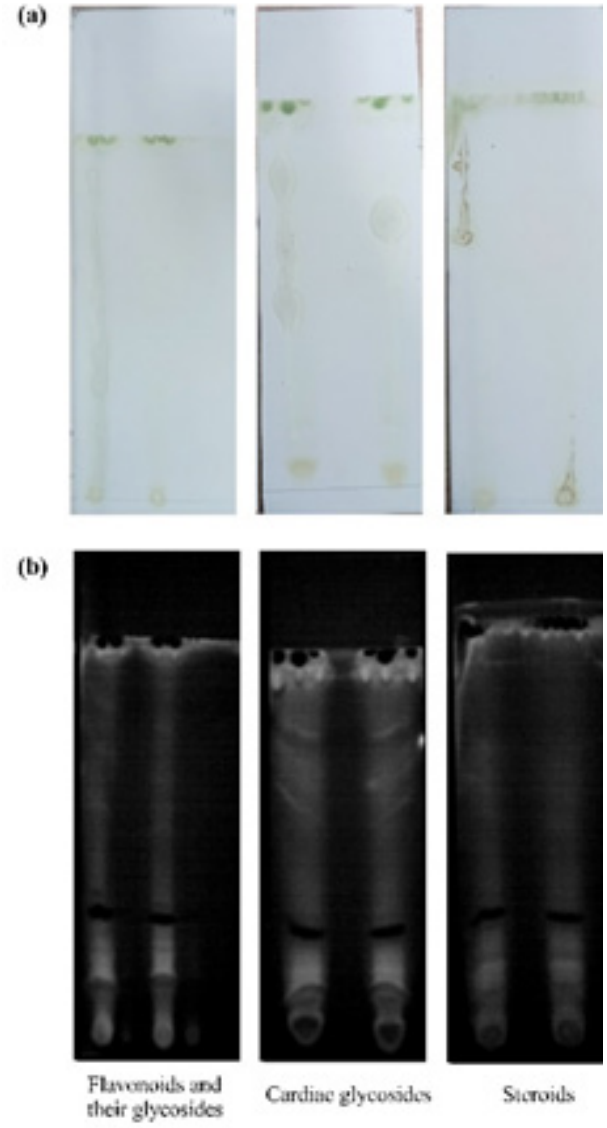

Figure 4) *Glass TLC profiling of methanolic Ct extract for various phytochemicals (a) Visualization through naked eye (b) Visualization through Gel-Doc system*

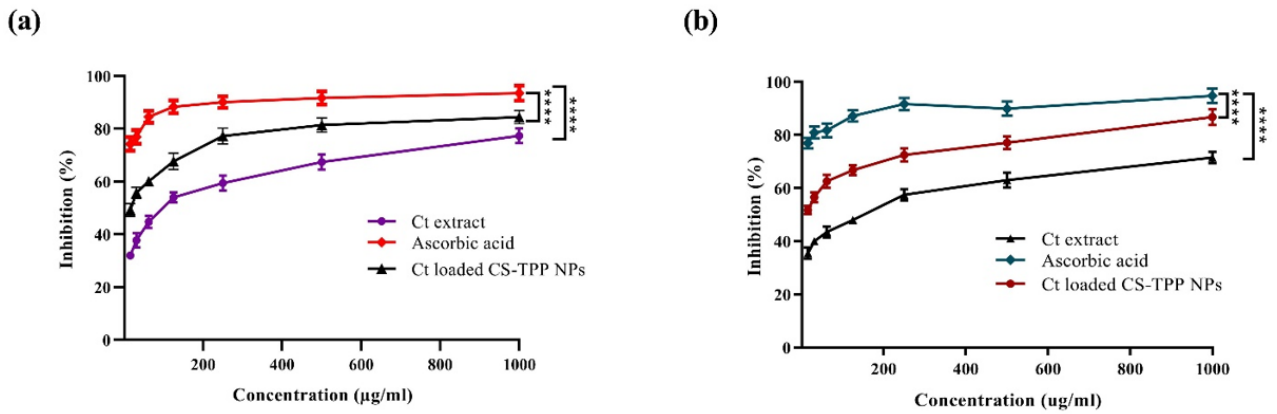

Figure 5) *Antioxidant activity of Ct extract and Ct loaded CS-TPP nanoparticles. (a) DPPH radical scavenging activities of various concentrations of Ct extract, Ct loaded CS-TPP NPs, and positive control (Ascorbic acid) (b) Hydrogen peroxide radical scavenging activity of the Ct extract, Ct loaded CS-TPP NPs, and ascorbic acid. Ct loaded CS-TPP nanoparticles showed significant antioxidant activity ($p<0.0001$) as compared to Ct extract.*

Hydrogen peroxide radical scavenging assay

Anti-oxidant activity of a series of concentrations of methanolic Ct extract was measured by hydrogen peroxide scavenging assay. Results showed that a percentage inhibition of 88% was exhibited at a concentration of 1000 µg/ml indicating strong antioxidant activity. The IC_{50} value calculated was 14.22 µg/ml for the methanolic Ct extract. Figure 5b shows the anti-oxidant activity of methanolic Ct extract compared with standard ascorbic acid.

CS-TPP nanoparticle synthesis

CS-TPP nanoparticles, Ct-loaded and rhodamine conjugated Ct-loaded CS-TPP nanoparticles were synthesized employing the ionic gelation method. Appearance of a white milky suspension confirmed the interaction of amine group (+ve charge) of CS with the phosphate group (-ve charge) of TPP and hence, the synthesis of nanoparticles. The samples were lyophilized and kept at 4°C. The methanolic Ct extract was encapsulated efficiently in the nanoformulation as shown in Figure 6a. The percentage encapsulation efficiency was calculated to be 87%.

Characterization of nanoparticles

UV spectrophotometry

The UV spectra for the synthesized nanoparticles were recorded in the range of 100-400 nm (U-2900 UV-VIS Spectrophotometer - HITACHI High-Tech Science, Tokyo, Japan; λ=200-1100 nm). The shift in peaks was recorded for the confirmation of CS-TPP nanoparticle formation and Ct encapsulation. The peak for pure chitosan solution (0.1%) is visible at 340 nm, as shown in Figure 6b. The peaks for Ct-loaded CS-TPP nanoparticles is visible at 340 nm and 327 nm. The second peak at 327 nm confirms the presence of Ct extract. Thus, these results confirm the synthesis of Ct loaded CS-TPP nanoparticles.

Fourier transform infra-red analysis (FTIR)

FTIR analysis was performed to confirm the synthesis of nanoparticles (4000-400/ cm using FTIR Spectrophotometer, equipped with software OMNIC™ version 6.0 a; Thermo Fisher Scientific). Figure 6c shows the absorption spectra of pure chitosan, CS-TPP nanoparticles, Ct extract and Ct loaded CS-TPP nanoparticles.

The FTIR spectra for pure chitosan showed characteristic absorption peak at 3332 cm^{-1} because of the stretching vibration in O–H group of pyranose ring and N–H group of amine group. The peak observed at 1630 cm^{-1} indicates the stretching vibrations in C=O bond in amide groups. The peak visible at 1344 cm^{-1} corresponds to the –C–C ring stretching vibrations, and pyrimidine compound vibrations

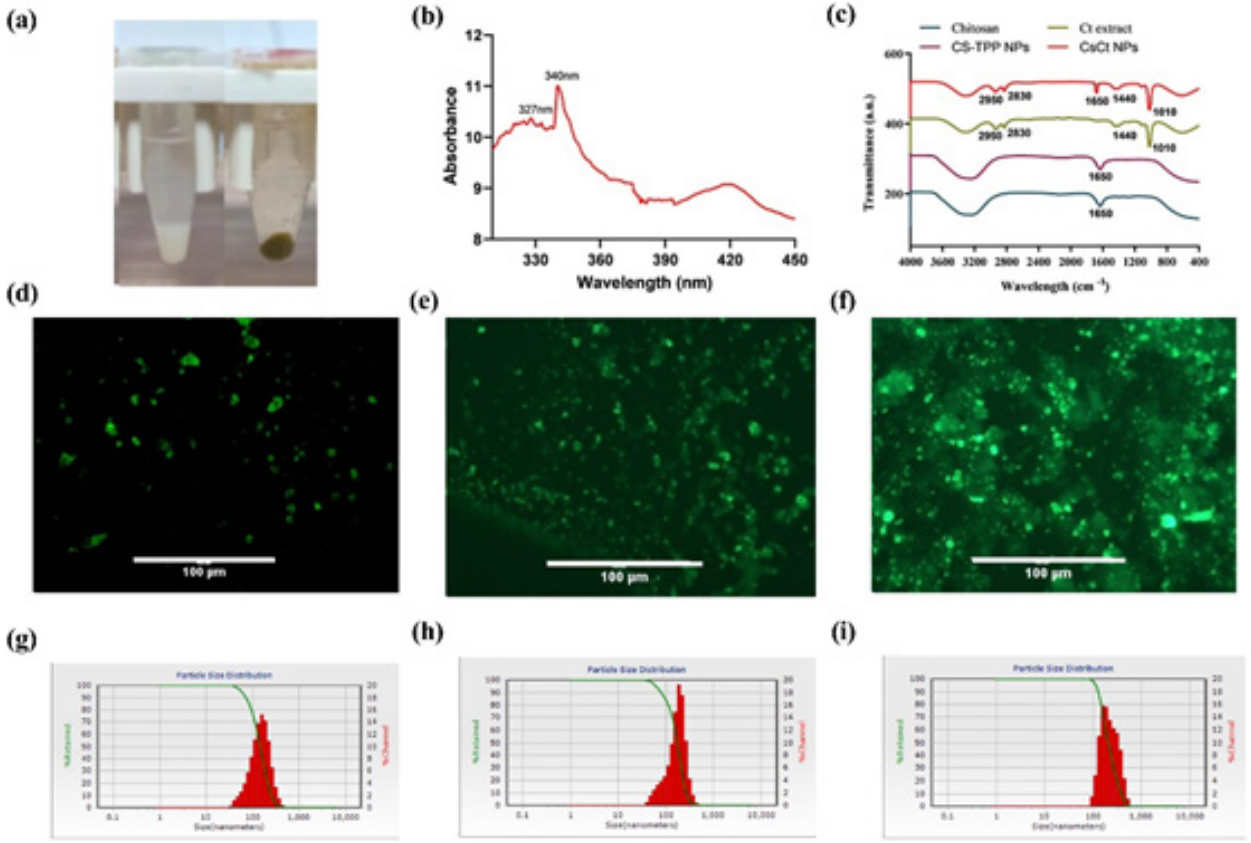

Figure 6) *Characterization of Ct loaded CS-TPP nanoparticles. a) Prepared CS-TPP and Ct loaded CS-TPP nanoparticles (0.1% w/v CS and 1% w/v TPP); b) UV spectra showing peak at 340 nm for chitosan and at 327 nm confirming the presence of Ct extract; c) FTIR spectra of Ct-loaded CS-TPP nanoparticles showing the appearance characteristic peaks similar to the spectra of Ct extract confirming the encapsulation of Ct in CS-TPP nanoparticles; d-f) Morphological appearance of nanoparticles before and after loading of Ct extract and visualized with Rhodamine dye; g-i) The particle size distribution of Ct extract, Ct loaded CS-TPP nanoparticles and rhodamine conjugated CS-TPP nanoparticles respectively measured by DLS showing size, zeta potential and polydispersity index values confirming good stability of the prepared nanoparticles.*

respectively. The absorption peak at 1289 cm^{-1} was due to N–H vibration in amide group. The FTIR spectra of CS-TPP nanoparticles showed the characteristics peaks at 3332 cm^{-1} and 1640 cm^{-1}. Absorption peak shift from 1630 cm^{-1} in the spectra of pure chitosan to 1640 cm^{-1} in the spectra of CS-TPP nanoparticles confirms the synthesis of nanoparticles.

The FTIR spectra of Ct extract showed absorption peaks at 3332 cm^{-1}, 1010 cm^{-1}, 1130 cm^{-1}, 1440 cm^{-1}, 2830 cm^{-1} and 2950 cm^{-1}. The FTIR spectra for Ct-loaded CS-TPP nanoparticles showed characteristic peaks at 3332 cm^{-1}, 1640 cm^{-1} and 1010 cm^{-1}. The appearance of absorption peaks at 1010 cm^{-1}, 1130 cm^{-1}, 1440 cm^{-1}, 2830 cm^{-1} and 2950 cm^{-1} in the spectra of Ct-loaded CS-TPP nanoparticles, similar to the spectra of Ct extract confirms the encapsulation of Ct in the nanoparticles.

Particle imaging

The morphological characteristics of nanoparticles were observed using cell imager (Evos® FL Cell Imaging System; Thermo Fisher Scientific, MA, USA). The images, as shown in Figures 6d and 6f, correlate with the DLS results, showing irregular shaped spherical nanoparticles. With the loading of the drug, the size of the nanoparticles has decreased which is consistent with the DLS results.

Measurement of size and zeta potential using dynamic light scattering

Particle size measurement of CS-TPP nanoparticles, Ct loaded CS-TPP nanoparticles and rhodamine conjugated CS-TPP nanoparticles by dynamic light scattering (DLS) showed 187 ± 4.583 nm, 140 ± 1.528 nm and 142 ± 3.334 nm respectively, as shown in Figures 6g to 6i. The zeta potential values were +44.5 ± 0.37mV, +59.5 ± 0.61mV and +61.5 ± 0.56mV respectively, confirming good stability of the prepared nanoparticles. After loading of the drug, the zeta potential value increased. This can be attributed to the higher interaction between the Ct extract and the nanoparticles. The prepared nanoparticles had a narrow size distribution with a polydispersity index less than or equal to 1.0.

Stability Study

The storage stability of the nanoformulations, with and without the loading of Ct extract, at 4˚C was evaluated. Stability studies showed that these formulations were stable up to 3 months retaining their initial size (183.66 to 206.66 ± 4.583 nm) , zeta potential (44.5 to 61.2 ± 0.37mV) and polydispersity index less than 1. Therefore, these prepared nano-formulations could be a promising candidate for application on cancer cells.

Biocompatibility study

It is evident from Figure 7, that with the increase in concentration, the RBC inhibition potential also increases. The percentage inhibition of the Ct extract was found to be less than 5% at minimum concentrations of 15.62 µg/ml, 31.25 µg/ml and 62.5 µg/ml. For the Ct loaded CS-TPP nanoparticles, the percentage inhibition was found to be less than or equal to 5% for concentrations of 15.62 µg/ml, 31.25 µg/ml, 62.5 µg/ml and 125 µg/ml. Hence, the prepared nano-formulation is safe to use at lower concentrations.

Cellular uptake

Cellular uptake of Ct loaded CS-TPP nanoparticles by triple negative cells was studied by visualizing the fluorescence of Rhodamine dye using cell imager (Evos imager (Evos® FL Cell Imaging System; Thermo Fisher Scientific, MA, USA). The samples were incubated for 24 hour and then fluorescent images were taken showing the uptake and retention of the nanoformulation by the cancer cells. However, the control cells showed no fluorescence, further validating the study Figures 8a to 8c.

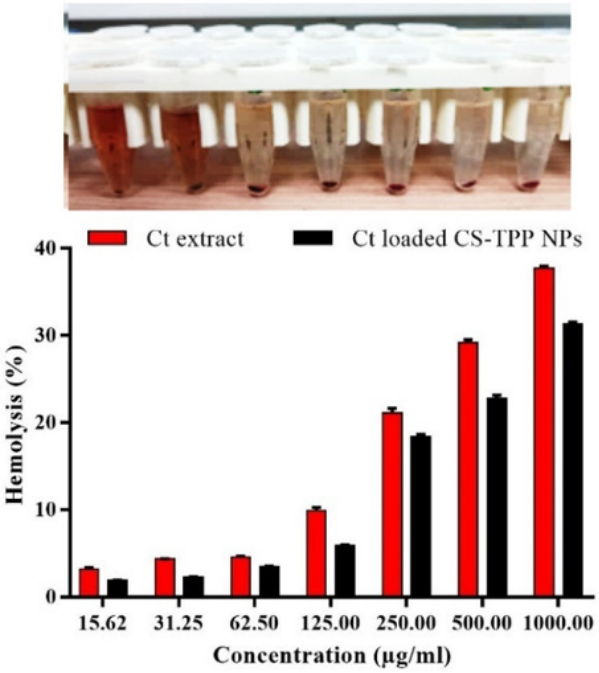

Figure 7) *Biocompatibility study of Ct extract and Ct-loaded CS-TPP nanoparticles. Physical observation after centrifugation and result analysis indicated that CS TPP nanoparticles loaded with Ct showed low haemolytic activity i.e. less than 5% up to 125 µg/ml of concentration compared to Ct extract alone.*

***In vitro* anticancer effect**

The cytotoxic effect of Ct extract and Ct loaded CS-TPP nanoparticles was tested against triple negative breast cancer cell lines at a concentration range of 0.156 to 2 µg/ml via MTT assay. The percentage cell viability of Ct extract and Ct loaded CS-TPP nanoparticles is shown in Figure 8d. It is clearly evident that the encapsulation of Ct extract in polymeric nanoparticles significantly increased the inhibition effect on the breast cancer cells from 30-40% for Ct extract alone to almost 75% for the Ct loaded nanoformulation. The IC_{50} of growth inhibition is 122.3 µg/ml for Ct extract and 14.39 µg/ml for Ct loaded CS-TPP nanoparticles.

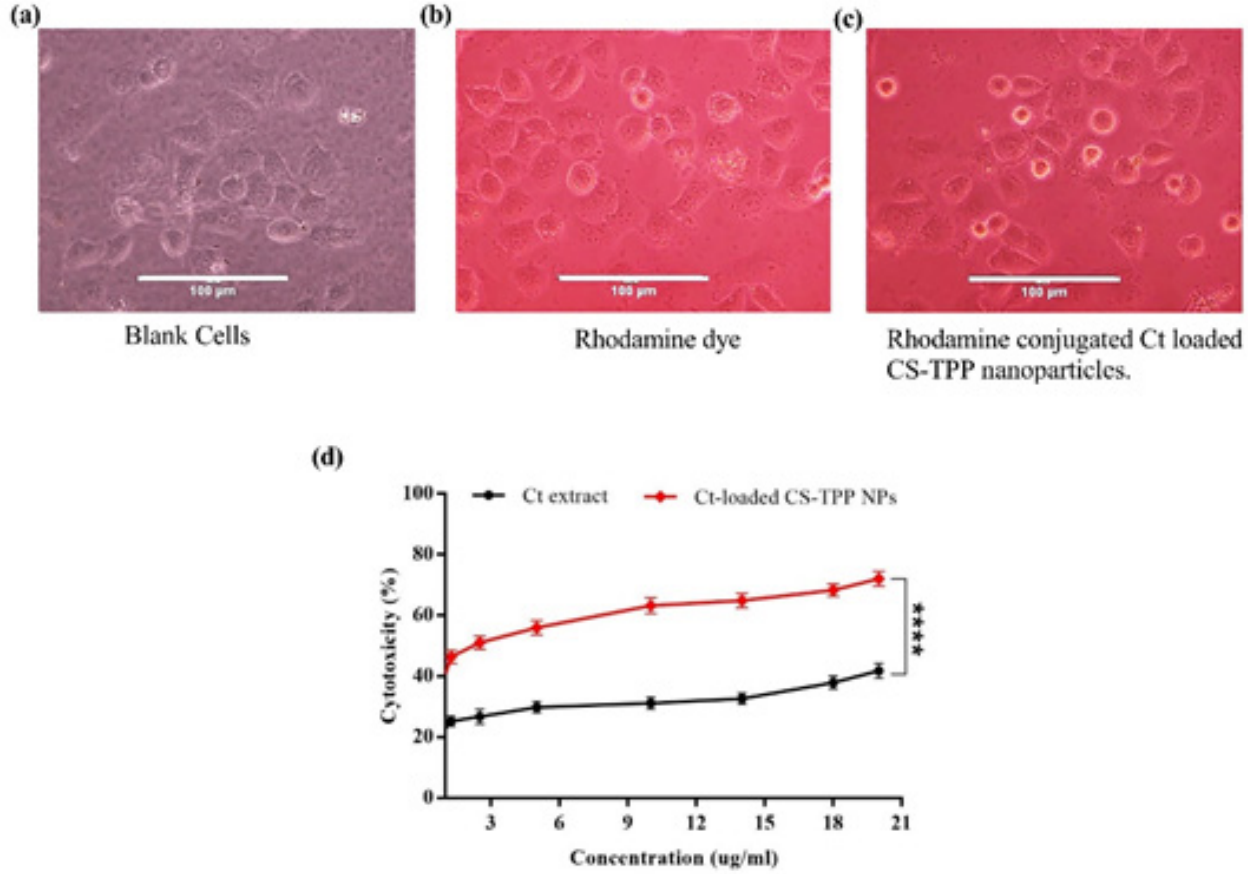

Figure 8) *Cellular uptake and cytotoxicity study of rhodamine conjugated nanoparticles in cancer cells. (a-c) Cell uptake of nanoparticles after 6 hours in cancer cells. The fluorescence intensity of rhodamine-loaded nanoparticles showed maximum cell uptake compared to Ct extract alone (d) CS-TPP nanoparticles containing Ct extract showed approximately 75% cytotoxicity on triple-negative breast cancer cells after 24 hours of treatment compared to Ct extract alone (30-40% cytotoxicity).*

Discussion

In the current study, Ct extract was successfully incorporated into CS-TPP nanoparticles through ion gelation method. The Ct loaded CS-TPP nanoparticles demonstrated a uniform size distribution with good stability for up to 3 months. Zeta potential is an important criteria to evaluate the stability of nanoparticles and their interaction with the cell membranes. Generally, nanoparticles exhibiting a zeta potential value higher than or equal to 30mV are considered stable [42]. The free primary amine group in chitosan may undergo ionization in a colloidal solution to form $-NH_3^+$, resulting in an overall positive zeta potential [43]. The zeta potential value, after the loading of Ct extract, has increased from +44.5mV to +59.5mV. This can be attributed to the higher interaction between the Ct extract and the CS-TPP nanoparticles.

Phytochemical study of the Ct extract confirmed the presence of medicinally important constituents such as tannins, cardiac glycosides, flavonoids and steroids. The qualitative tests for terpenoids and phenol came out to be negative. Previous studies also revealed the presence of these phytochemicals in the Ct extract. The presence of these secondary metabolites, specifically cardiac glycosides makes this plant a promising anti-cancer drug as reported earlier [44,45].

The percentage free radical scavenging values were found to be 86.25% (IC_{50}=140.1 µg/ml) and 88% (IC_{50}=14.22 µg/ml) at a concentration of 1000 µg/ml for DPPH scavenging assay and H_2O_2 radical scavenging assay respectively.

Similar study was conducted in which methanolic Ct extract showed strong anti-oxidant activity of over 80% inhibition at a concentration of 500 µg/ml [46]. Other studies also confirm the strong anti-oxidant potential of methanolic Ct extract [47].

In vitro hemolytic assay for Ct extract and Ct loaded CS-TPP nanoparticles was performed to determine the safe range of dose concentration for testing against cancer cells. The RBC inhibition potential increases with the increase in concentration. The percentage inhibition was found to be less than or equal to 5% for concentrations of 15.62 µg/ml, 31.25 µg/ml, 62.5 µg/ml and 125 µg/ml. Hence, the prepared nano formulation was safe to use at lower concentrations. These results are in agreement with another study where the anti-hemolytic potential of Caralluma species was evaluated. A dose-dependent inhibition was observed in the concentration range of 50 -1000 µg/ml and 10-250 µg/ml. The phytoconstituents in the Caralluma extract scavenge the generated free radicals hence, preventing the red blood cells from membrane damage caused by oxidative stress [48].

The Ct extract and Ct loaded CS-TPP nanoparticles were treated against triple negative breast cancer cell lines for the evaluation of cytotoxicity. The IC_{50} of growth inhibition is 122.3 µg/ml for free Ct extract and 14.39 µg/ml for Ct loaded CS-TPP nanoparticles. The nano-formulation exhibited up to 75% cytotoxic effect while that of Ct extract was found to be 30-40%. These results showed that CS-TPP nanoparticles, when loaded with Ct extract led to a significantly higher viability reduction of cancer cells ($P<0.0001$). The substantial anticancer effect of Ct loaded CS-TPP nanoparticles may be because of better internalization of the nanoparticle system as compared to that of the free extract. Also, the positive charge on the surface of chitosan nanoparticles greatly increases its chances of internalization in negatively charged cancer cells [49,50].

In agreement to these results, a study was performed by where Russelioside A, a pregnane glucoside from Ct exhibited a considerable inhibition effect on the metastatic ability of breast cancer cells. This shows the potential of Ct extract to inhibit the cell viability of cancer cells. A recent study has reported the effect of Ct capped AgNPs and Ct capped AgNPs hybridized with poly(ethylene glycol) methacrylate against prostatic adenocarcinoma (PC-3) cell lines. The results confirmed the significant anticancer potential (IC_{50}=38 µg/ml and 34 µg/ml respectively) of Ct capped metallic nanoparticles [51]. Other species of Caralluma such as *Caralluma acutangula* have also been reported for their excellent cytotoxic and anticancer activity against hepatocellular carcinoma (HEPG2) and breast cancer (MCF-7) cells [52]. Another study to evaluate the anticancer potential of methotrexate loaded chitosan nanoparticles was performed in HeLa cells. The results showed a considerable cell growth inhibition effect (42.72%) after treatment for 72hour [53].

Conclusion

We have reported the synthesis of chitosan nanoparticles, loaded with pharmacologically endowed Ct extract exhibiting significant anti-oxidant potential. The findings of the current study showed that the methanolic Ct extract and the Ct loaded nanoformulation exhibited significant anti-cancer potential with 30-40% inhibition (IC_{50}=122.3 µg/ml) and up to 75% inhibiton (IC_{50}=14.39 µg/ml) respectively. The dosage was found safe at lower concentrations up to 125 µg/ml via hemolytic assay. The results conclusively showed that the anti-cancer activity of Ct extract against triple negative breast cancer cells is enhanced by its loading in the CS-TPP nanoparticles, authenticating its use as an anti-cancer nanodrug. Hence, Ct extract in conjugation with nanoparticles proved to be an

effective combinational therapy against breast cancer cells since it allowed for a more targeted and biocompatible drug delivery system with higher potency and significance. Our findings may pave the way for further studies on the concentration-dependent effect of Ct extract on cancer cells to yield even more efficient results. Moreover, this study suggests possible leads for researchers to study the use of Ct loaded nanoformulations against other cancer cell lines.

Acknowledgements

We thank National Institute of Laser and Optronics (NILOP), Islamabad, Pakistan for facilitation and Lahore University of Management Sciences (LUMS), Lahore, Pakistan for providing triple negative breast cancer cell lines as gift courtesy.

References

1. Patra JK, Das G, Fraceto LF, et al. Nano based drug delivery systems: recent developments and future prospects. J Nanobiotechnology. 2018;16:71.
2. Li C, Wang J, Wang Y, et al. Recent progress in drug delivery. Acta Pharm Sin B. 2019;9:1145-62.
3. Ahmad MZ, Rizwanullah M, Ahmad J, et al. Progress in nanomedicine-based drug delivery in designing of chitosan nanoparticles for cancer therapy. Int J Polym Mater Polym Biomater. 2022;71:602-23.
4. Chavan T, Muttil P, Kunda NK. Introduction to nanomedicine in drug delivery. In: Muttil P, Kunda N. (eds) Mucosal Delivery of Drugs and Biologics in Nanoparticles, Springer, Cham. 2020.
5. Barik R, Sugunan S, Pal A. Nanotechnology-based drug delivery of phytotherapeutics: herbal drugs and nanotechnology. In: Verma S, Verma S. (eds.) Advancements in Controlled Drug Delivery Systems, IGI Global, Pennsylvania, USA. 2022;pp.73-96.
6. Bandyopadhyay A, Roy B, Shaw P, et al. Cytotoxic effect of green synthesized silver nanoparticles in MCF7 and MDA-MB-231 human breast cancer cells *in vitro*. The Nucleus. 2020;63:191-202.
7. Ovais M, Khalil AT, Raza A, et al. Green synthesis of silver nanoparticles via plant extracts: beginning a new era in cancer theranostics. Nanomedicine. 2016;12:3157-77.
8. Chun SC, Chandrasekaran M. Chitosan and chitosan nanoparticles induced expression of pathogenesis-related proteins genes enhances biotic stress tolerance in tomato. Int J Biol Macromol. 2019;125:948-54.
9. Metselaar JM, Lammers T. Challenges in nanomedicine clinical translation. Drug Deliv Transl Res. 2020;10:721-25.
10. Pedziwiatr-Werbicka E, Milowska K, Dzmitruk V, et al. Dendrimers and hyperbranched structures for biomedical applications. Eur Polym J. 2019;119:61-73.
11. Wang G, Li R, Parseh B, et al. Prospects and challenges of anticancer agents' delivery via chitosan-based drug carriers to combat breast cancer: a review. Carbohydr Polym. 2021;268:118192
12. Kanwal U, Bukhari NI, Rana NF, et al. Doxorubicin-loaded quaternary ammonium palmitoyl glycol chitosan polymeric nanoformulation: uptake by cells and organs. Int J Nanomedicine. 2018;14:1-15.
13. Rostami E. Progresses in targeted drug delivery systems using chitosan nanoparticles in cancer therapy: a mini-review. J Drug Deliv Sci Technol. 2020;58:101813.
14. Ashrafizadeh M, Ahmadi Z, Mohamadi N, et al. Chitosan-based advanced materials for docetaxel and paclitaxel delivery: recent advances and future directions in cancer theranostics. Int J Biol Macromol. 2020;145:282-300.

15. Naskar S, Sharma S, Kuotsu K. Chitosan-based nanoparticles: an overview of biomedical applications and its preparation. J Drug Deliv Sci Technol. 2019;49:66-81.

16. Faisal MS, Hayat W, Inayat A, et al. Comparison of *Caralluma tuberculata* with metformin for anti-diabetic activity: an animal study. J Islamabad Med Dent Coll. 2019;8:34-9.

17. Ali A, Mohammad S, Khan MA, et al. Silver nanoparticles elicited *in vitro* callus cultures for accumulation of biomass and secondary metabolites in *Caralluma tuberculata*. Artif Cells Nanomed Biotechnol. 2019;47:715-24.

18. Anwar R, Rabail R, Rakha A, et al. Delving the role of *Caralluma fimbriata*: an edible wild plant to mitigate the biomarkers of metabolic syndrome. Oxid Med Cell Longev. 2022;2022:5720372.

19. Ouassou H, Bouhrim M, Kharchoufa L, et al. *Caralluma europaea* (Guss) NE Br: a review on ethnomedicinal uses, phytochemistry, pharmacological activities, and toxicology. J Ethnopharmacol. 2021;273:113769.

20. Shahrajabian MH, Sun W, Cheng Q. The importance of flavonoids and phytochemicals of medicinal plants with antiviral activities. Mini Rev Org. 2022;19:293-318.

21. Ali A, Ahmad I, Raja NI, et al. Plant *in vitro* cultures: a promising and emerging technology for the feasible production of antidiabetic metabolites in *Caralluma tuberculata*. Front Endocrinol (Lausanne). 2022;13:1029942.

22. Ahmad T, Malik MN, Mushtaq MN, et al. Evaluation of antihypertensive effect of aqueous methanol extract of *Caralluma tuberculata* NE Br in sprauge dawley rats. Trop J Pharm Res. 2015;14:455-62.

23. Rahman S, Zahid M, Khan AA, et al. Hepatoprotective effects of walnut oil and *Caralluma tuberculata* against paracetamol in experimentally induced liver toxicity in mice. Acta Biochim Pol. 2022;69:871-78.

24. Abdel-Sattar E, Ali DE. Russelioside B: a pregnane glycoside with pharmacological potential. Revista Brasileira de Farmacognosia. 2022;32:188-200.

25. Khan MA, Maqsood K, Uslu OS. *Caralluma tuberculata*-An important medicinal plant to be conserved. Biol Divers Conserv. 2022;12:189-96.

26. Sabra RT, Abdellatef AA, Abdel-Sattar E, et al. Russelioside A, a pregnane glycoside from C*aralluma tuberculate*, inhibits cell-intrinsic nf-κb activity and metastatic ability of breast cancer cells. Biol Pharm Bull. 2022;45:1564-71.

27. Ali M, Sherani S. Acute and sub-chronic toxicity assessment of *Caralluma tuberculata* plant collected from district Sherani of Balochistan, Pakistan. Pak-Euro Journal of Medical and Life Sciences. 2021;4:73-82.

28. Reddy D, Kumavath R, Barh D, et al. Anticancer and antiviral properties of cardiac glycosides: a review to explore the mechanism of actions. Molecules. 2020;25:3596.

29. Patergnani S, Danese A, Bouhamida E, et al. Various aspects of calcium signalling in the regulation of apoptosis, autophagy, cell proliferation, and cancer. Int J Mol Sci. 2020;21:8323.

30. Lin RC, Yang SF, Chiou HL, et al. Licochalcone A-induced apoptosis through the activation of p38MAPK pathway mediated mitochondrial pathways of apoptosis in human osteosarcoma cells *in vitro* and *in vivo*. Cells. 2019;8:1441.

31. Shubham S, Mishra R, Gautam N, et al. Phytochemical analysis of papaya leaf extract: screening test. EC Dent Sci. 2019;18:485-90.

32. Ahmad W, Singh S, Kumar S. Phytochemical screening and antimicrobial study of *Euphorbia hirta* extracts. J Med Plants Stud. 2017;5:183-6.

33. Oleszek W, Kapusta I, Stochmal A. 20TLC of triterpenes (Including Saponins). In: Hajnos MW, Sherma J, Kowalska T. (eds). Thin layer chromatography in phytochemistry. (1stedn), Taylor & Francis Groups, India. 2008;p.519.

34. Shah Hosseini SR, Safari R, Javadiyan SR. Evaluation antioxidant effects of Pullulan edible coating with watercress extract (*Nasturtiumn officinale*) on the chemical corruption of fresh beluga sturgeon fillet during storage in a refrigerator. Iran J Fish Sci. 2021;30:133-46

35. Brand-Williams W, Cuvelier ME, Berset C. Use of a free radical method to evaluate antioxidant activity. LWT Food Sci Technol. 1995;28:25-30.

36. Christodoulou MC, Orellana Palacios JC, Hesami G, et al. Spectrophotometric methods for measurement of antioxidant activity in food and pharmaceuticals. Antioxidants. 2022;11:2213.

37. Shafiei M, Jafarizadeh-Malmiri H, Rezaei M. Biological activities of chitosan and prepared chitosan-tripolyphosphate nanoparticles using ionic gelation method against various pathogenic bacteria and fungi strains. Biologia. 2019;74:1561-8.

38. Anwar N, Wahid J, Uddin J, et al. Phytosynthesis of poly (ethylene glycol) methacrylate-hybridized gold nanoparticles from *C. tuberculata*: their structural characterization and potential for *in vitro* growth in banana. *In Vitro* Cell Dev Biol. 2021;57:248-60.

39. Rehman M, Raza A, Khan JA, et al. Laser responsive cisplatin-gold nano-assembly synergizes the effect of cisplatin with compliance. J Pharm Sci. 2021;110:1749-60.

40. Hashemi M, Shamshiri A, Saeedi M, et al. Aptamer-conjugated PLGA nanoparticles for delivery and imaging of cancer therapeutic drugs. Arch Biochem Biophys. 2020;691:108485.

41. Sarwar U, Naeem M, Nurjis F, et al. Ultrasound-mediated *in vivo* biodistribution of coumarin-labeled nanotheranostic system. Nanomedicine. 2022;17:1909-27.

42. Pochapski DJ, Carvalho dos Santos C, Leite GW, et al. Zeta potential and colloidal stability predictions for inorganic nanoparticle dispersions: effects of experimental conditions and electrokinetic models on the interpretation of results. Langmuir. 2021;37:13379-89.

43. Ahmad MZ, Sabri AHB, Anjani QK, et al. Design and development of levodopa loaded polymeric nanoparticles for intranasal delivery. Pharmaceuticals. 2022;15:370.

44. Shazmeen N, Nazir M, Riaz N, et al. *In vitro* antioxidant and enzyme inhibitory studies, computational analysis and chemodiversity of an emergency food plant *Caralluma edulis* (Edgew.) Benth. ex Hook. f: a multifunctional approach to provide new ingredients for nutraceuticals and functional foods. Food Biosci. 2022;50:102097.

45. Farouk AE, Ahamed NT, AlZahrani O, et al. Antimicrobial activity of *Caralluma quadrangula* (Forssk) NE Br latex from Al-ShafaTaif, Kingdom of Saudi Arabia. Int J Curr Microbiol App Sci. 2016;5:284-98.

46. Poodineh J, Nakhaee A. *In vitro* antioxidant and anti-lipid peroxidation activities of hydroalcoholic extracts of *Caralluma tuberculata,* root and aerial parts. Jundishapur J Nat Pharm Prod. 2019;14:e69685.

47. Dra LA, Sellami S, Rais H, et al. Antidiabetic potential of *Caralluma europaea* against alloxan-induced diabetes in mice. Saudi J Biol Sci. 2019;26:1171-8.

48. Bhat SH, Ullah MF, Abu-Duhier FM. Anti-hemolytic activity and antioxidant studies of *Caralluma quadrangula:* potential for nutraceutical development in cancers and blood disorders. Int J Pharm Res Allied Sci. 2019;8:121-9.

49. Rahimi M, Mir SM, Baghban R, et al. Chitosan-based biomaterials for the treatment of bone disorders. Int J Biol Macromol. 2022;215:346-67.

50. Ai J, Liao W, Ren ZL. Enhanced anticancer effect of copper-loaded chitosan nanoparticles against osteosarcoma. RSC Adv. 2017;7:15971-7.

51. Anwar N, Khan A, Shah M, et al. Hybridization of green synthesized silver nanoparticles with poly (ethylene glycol) methacrylate and their biomedical applications. PeerJ. 2022;10:e12540.

52. Al-Faifi ZI, Masrahi YS, Aly MS, et al. *In vitro* anticancer activity of *Caralluma acutangula* (Decne.) N.E.Br. Extract. Int J Pharm Sci Rev Res. 2016;38:59-63.

53. Mazzotta E, De Benedittis S, Qualtieri A, et al. Actively targeted and redox responsive delivery of anticancer drug by chitosan nanoparticles. Pharmaceutics. 2019;12:26.

ISSN 2816-573X

Supplementary Data Appendix

Material and Methods

Materials

The materials and chemicals used or this study included; Acetic acid, ascorbic acid, boric acid, carbon dioxide (CO_2), chitosan (molecular weight >150kDa), chloroform, DAPI (4',6-diamidino-2-phenylindole), Dulbecco's Modified Eagle Media (DMEM), penicillin-streptomycin, DPPH (1, 1-diphenyl-2-picryl-hydrazyl), ethanol, ethyl acetate, fetal bovine serum (FBS), ferric chloride, hydrogen peroxide, methanol, MTT (3-(4,5-dimethylthiazol-2-yl)-2,5-diphenyl-2H-tetrazolium bromide), oxalic acid, paraformaldehyde, penicillin, phosphate buffered-saline (PBS), potassium hydroxide, rhodamine dye, sodium tripolyphosphate (TPP), sulfuric acid, Triton X-100.

Plant collection and extraction

The whole plant was shade-dried and grounded. The powdered sample was extracted in a ratio of 1:5 in three solvents; Methanol (MeOH), Ethanol (EtOH), and Chloroform ($CHCl_3$). The extracts were then placed in a drying oven for 48 hours. Prepared extracts were then collected, weighed, and stored for further analysis. Ct extracts possessed colour variations ranging from black to dark green. Most of the fractions were non-sticky.

Qualitative Phytochemical Tests

Thin layer chromatography (TLC)

Ct extract (2 mg/ml) was used. The glass TLC plates (silica gel coated, L × W 20 cm × 20 cm) were cut into equal sizes. The sample was loaded with the help of capillary tubes. The extract was tested for different mobile phase combinations for a better understanding of bands. The solvent system used was Chloroform: Methanol (7:3) and Ethyl acetate: Methanol: Water (81:11:8) respectively. The prepared TLC plates were then placed inside the TLC jars and the mobile phase was allowed to run. When the solvents reached the top line of the TLC plates, the plates were removed and air-dried for few minutes followed by spraying with visualizing agents and observed under UV.

For flavonoids and their glycosides, the dried TLC plate was sprayed with a mixture of 3% boric acid and 10% oxalic acid solutions. These solutions were prepared separately, mixed, and kept for a few minutes before spraying. For cardiac glycosides, the dried TLC plate was sprayed with the mixture of 10% KOH and 50% methanol solutions. These solutions were prepared separately, mixed, and kept for a few minutes before spraying. For steroids, the dried TLC plate was sprayed with 10% H_2SO_4 solution.

Antioxidant assays

DPPH (1, 1-diphenyl-2-picryl-hydrazyl) free radical scavenging assay

To prepare the stock solution, 0.24g of DPPH was dissolved in 100ml of methanol and stored at 20ºC for use. Further dilution was done by adding methanol to the solution until the absorbance was optimized (0.8-0.9) at 517 nm (U-2900 UV-VIS Spectrophotometer - HITACHI High-Tech Science, Tokyo, Japan; λ=200-1100 nm). In various concentrations, 100µl of Ct extract solution was added to 900µl of DPPH. This was followed by incubation in the dark for 30min at room temperature. A similar procedure was performed for Ct loaded CS-TPP nanoparticles. Ascorbic acid was run as standard.

Hydrogen peroxide radical scavenging assay

Stock solution (2mM H_2O_2) was prepared in phosphate buffered-saline PBS (50mM, pH 7.4). A series of seven concentrations of Ct extract was added and the overall volume was made up to 5ml by the addition of H_2O_2 solution. The

absorbance was measured at 230 nm (U-2900 UV-VIS Spectrophotometer - HITACHI High-Tech Science, Tokyo, Japan; λ=200-1100 nm) against a blank containing only PBS. A similar procedure was performed for the Ct loaded CS-TPP nanoparticles. Ascorbic acid was used as a reference.

Characterization of nanoparticles

The UV spectra for the synthesized nanoparticles were recorded in the range of 100-400 nm (U-2900 UV-VIS Spectrophotometer - HITACHI High-Tech Science, Tokyo, Japan; λ=200-1100 nm). The shift in peaks was recorded for the confirmation of CS-TPP nanoparticle formation and Ct encapsulation. FTIR analysis was done to confirm the synthesis of nanoparticles. The samples were screened (4000-400/ cm using FTIR Spectrophotometer, equipped with software OMNIC™ version 6.0 a; Thermo Fisher Scientific). Particle imaging to visualize the morphological characteristics of nanoparticles was achieved using a cell imager (Evos® FL Cell Imaging System; Thermo Fisher Scientific, MA, USA). The images for the nanoformulation were taken at a magnification of 40×. Dynamic Light Scattering (DLS) was used for the measurement of particle size, polydispersity index (PDI), and zeta potential of nanoparticles (DLS; Microtrac Nanotrac Wave II, PA, USA). Each sample was analysed three times at 25°C and 90°C scattering angle. Distilled water was used as a reference.